

INHERENT DESIGN MARGINS IN STRUCTURES  
SUBJECTED TO PULSE TYPE LOADS

SDAR-78-02

MAY 1978

Prepared by: S Ranganath  
S. Ranganath, Manager  
Stress & Fracture Analysis

Reviewed by: Subramanian  
C. V. Subramanian  
Dynamic & Seismic Analysis

Approved by: D. Gilman  
D. Gilman, Manager  
Dynamic & Seismic Analysis

24299

7810270061

# ABSTRACT

The inherent safety margin in nuclear structures subjected to dynamic loading and designed to meet ASME Code limits is evaluated using a simple single degree of freedom system. Analysis is performed for linear elastic behavior and elastic-plastic behavior using a bi-linear stress-strain curve. It is shown that when plasticity effects are included the peak load to failure is significantly higher than that obtained by linear elastic analysis alone. It is, therefore, concluded that for structures designed to meet ASME Code limits, the inherent safety margin is significantly higher for dynamic pulse loads than for static loads.

## 1. INTRODUCTION

Nuclear pressure vessel structures are often subjected to dynamic loads which last only for a short duration. Examples of such loads are safety relief valve loads, seismic loads, etc. which are generally classified under Class C and Class D conditions (Emergency and Faulted conditions). The ASME Code prescribes allowable limits for these Class C and D loads. In comparing the applied loads against the code limits, the dynamic analysis is generally performed assuming elastic behavior. This takes into account the effects of inertia and is adequate for applied loads which lead to elastic stresses. However, when large impulsive loads are applied on structures which lead to some plastic deformation, the use of elastic dynamic analysis may be over-conservative since the comparison with the code limits are based on applied stresses. In reality some yielding can be tolerated and, therefore, the actual stresses in the structure are likely to be lower than the values calculated by elastic analysis. This can be shown by performing an elastic-plastic dynamic analysis of the structure. However, such an analysis is not practical for complex structures involving several degrees of freedom. Nevertheless, valid conclusions can be obtained by comparing the results of elastic-plastic analysis and linear elastic analysis for a simple single degree of freedom model for impulsive loads. The purpose of this report is to demonstrate the conservatism introduced due to the use of elastic dynamic analysis and to estimate the magnitude of the inherent safety margin that exists in present practice. Elastic analysis is performed for a triangular pulse load with different periods using a single degree of freedom model. The maximum force in the structure and the corresponding displacement are computed for a given peak load and pulse duration. Elastic-plastic analysis is performed using a bi-linear approximation to the experimental stress-strain curve. The solution to the governing differential equation is obtained numerically using a finite difference approach and the results are compared with the corresponding values from elastic analysis. Based on this comparison the additional safety margin due to nonlinear material

behavior can be determined.

## 2. LINEAR ELASTIC EVALUATION

In order to understand the response of structures to impulsive loading a simple single degree freedom spring-mass system of the type shown in Fig. 1 is selected. The applied force is a function of time  $F(T)$ . For the results presented here, a triangular pulse of the type shown in Figure 1 is employed. However, the numerical method developed here is completely general and can be used for an arbitrary pulse shape.

The equation of equilibrium is;

$$M \ddot{X} + K X = F(T) \quad (1)$$

where      $M$  = mass of the structure  
            $K$  = stiffness, constant for elastic behavior  
            $X$  = displacement and  
            $F(T)$  = applied dynamic load

For a triangular pulse load of peak value  $P$  and, duration  $T_0$  the forcing function is given by

$$F(T) = \begin{cases} 2PT/T_0 & \text{for } 0 \leq T \leq T_0/2 \\ 2P(T_0 - T)/T_0 & \text{for } T_0/2 \leq T \leq T_0 \\ 0 & \text{for } T \geq T_0 \end{cases}$$

Equation (1) can be simplified by introducing the following non-dimensional variables;

$$x = \frac{X}{X_s} \quad \text{where } X_s = \text{maximum static displacement} = \frac{P}{K}$$

$$t = wT \text{ and } t_0 = wT_0 \quad \text{where } w = \sqrt{K/M} = 2\pi f$$

$f$  = natural frequency of the system

$$T_N = \frac{1}{f} = \text{natural period of the system.}$$

Following substitution the equations reduce to the following non-dimensional form:

$$\frac{d^2 x}{dt^2} + x = f(t) \quad \text{Where}$$

$$f(t) = \begin{cases} 2t/t_0 & 0 \leq t \leq t_0/2 \\ 2(t_0 - t)/t_0 & t_0/2 \leq t \leq t_0 \\ 0 & t \geq t_0 \end{cases} \quad -(2)$$

The initial conditions are  $x = 0$  and  $\frac{dx}{dt} = 0$  at  $t=0$ .

Closed form solutions can be obtained for the elastic case during the rising period of the pulse (i.e.,  $t \leq t_0/2$ ) as

$$x = 2(t - \sin t)/t_0$$

However, the closed form solution for the unloading portion of the pulse becomes complicated. A more general solution can be obtained by numerically integrating the equation using a second order accurate difference method. The numerical solution to Equation (2) can be obtained using a centered difference scheme of the type shown in Figure 2 and given by

$$\frac{x(i+1) - 2x(i) + x(i-1))}{\Delta t^2} + x(i) = F[(i-1)\Delta t] \quad -(3)$$

where  $x(1)$  is the solution at time  $t = 1\Delta t$  and  $\Delta t$  is the time increment.

The initial conditions are given by

$$x(1) = 0$$

$$\dot{x}(1) = 2(\Delta t - \sin \omega \Delta t)/t_0$$

Knowing the solution at  $1$  and  $(1-1)$ , the solution at  $(1+1)$  can be calculated from Equation 3. The elastic response of a single degree of freedom system to a triangular pulse load was calculated for different pulse durations using a computer program based on the above difference equations. Computations were performed up to one natural period  $T_N$  and each time step was taken equal to  $.005 T_N$ . Figure 3 shows a plot of the maximum non-dimensional displacement (which equals actual dynamic displacement/static displacement) as a function of non-dimensional pulse duration (i.e., pulse duration/natural period). As expected, for a given peak load the maximum displacement and the stress in the structure decrease as the pulse width is reduced. This is consistent with the expected dependence of the maximum displacement with the applied impulse. On the other hand, as the pulse duration approaches the natural period, the maximum dynamic displacement exceeds the static value and static analysis is no longer conservative for such cases. The elastic analysis presented here does not consider any viscous damping and some conservatism is built in as a result of this assumption.

### 3. ELASTIC-PLASTIC EVALUATION

In order to evaluate problems where the applied load is sufficient to cause plastic deformation in the structure, a bi-linear stress-strain curve (Fig. 4) was employed. A bi-linear fit to the minimum stress-strain curve for 304 stainless steel at  $550^\circ\text{F}$  (Fig. 5) was used for the calculations presented here. For the elastic-plastic analysis three different regimes must be considered which are:

- (i) elastic loading up to the yield point
- (ii) elastic-plastic loading beyond the yield point during which the deformation is governed by the slope of the plastic portion of the stress-strain curve, and
- (iii) unloading during which the behavior is elastic (until reversed yielding occurs).

The equations of motion for the three different regimes are as follows:

#### Elastic Loading

$$M \ddot{x} + Kx = F(t) \quad x < x_e$$

where  $x_e$  is the displacement (generalized strain) corresponding to the yield load (stress)  $P_e$ .

#### Elastic Plastic Loading

$$M \ddot{x} + P_e + K'(x - x_e) = F(t) \quad x_e < x < x_{max}$$

where  $K'$  = slope of the plastic portion of the stress-strain curve.  
and  $x_{max}$  = maximum displacement just prior to unloading.

This regime is valid as long as the displacement keeps increasing with time. Once unloading occurs, the material behavior becomes elastic.

#### Unloading

$$\ddot{x} + P_e + K'(x_{max} - P_e) + K(x - x_{max}) = F(t)$$

The above equations can be non-dimensionalized by the following substitutions:

$$x = \tilde{x} / x_e, \quad x_{max} = \tilde{x}_{max} / x_e$$

$$t = \omega t \quad \omega = 2\pi T / T_N, \quad p = F / P_e$$

$$\omega = \sqrt{K/M} \quad \text{and}$$

$\lambda = K'/K$  = ratio of the slopes of the plastic and elastic portions of the stress-strain curve.

The non-dimensionalized equations are:

$$\ddot{x} + x = f(t) \quad 0 \leq x \leq 1$$

$$\ddot{x} + \lambda x = f(t) + \lambda - 1 \quad 1 \leq x \leq x_{max}$$

$$\ddot{x} + x = f(t) + (x_{max} - 1)(1 - \lambda) \quad x \geq x_{max}$$

where

$$f(t) = \begin{cases} 2pt/t_0 & 0 \leq t \leq t_0/2 \\ 2p(t_0 - t)/t_0 & t_0/2 \leq t \leq t_0 \\ 0 & t \geq t_0 \end{cases}$$

The above equations can be integrated using the difference method described earlier. A computer program for solving the differential equations was developed. The program computes the displacement at each step and when the non-dimensional displacement is less than one, the elastic equations are used. When the displacement  $x$  exceeds one, the equations for elastic-plastic behavior are used. When the increment in  $x$  after a time step becomes negative, unloading occurs and the equations for elastic behavior are used. Computations were performed for time  $T$ , up to one natural period  $T_N$ . For the numerical examples presented here, the maximum displacements (or strains) were reached within the time range for which computations were made. Also, reversed yielding did not occur during this time range. The results of the numerical evaluation obtained using the stress-strain curve for 304 stainless steel are presented in Figure 6 for five different pulse durations. The maximum non-dimensional displacement is plotted as a function of applied load for the selected pulse duration. Because of the non-dimensionalization, the load versus displacement plot is also equivalent to applied stress versus maximum strain in the structure. From this plot the allowable maximum applied stress can be computed for a given maximum strain and pulse duration. For instance, if a strain of  $10\epsilon_y$  (for the 304 stainless steel stress-strain curve used here  $\epsilon_y = .075\%$ ) is the maximum allowable value for emergency conditions, (Class C), for a triangular pulse of duration  $0.1 T_N$ , the maximum allowable stress is 14.5 times the yield stress ( $\sigma_y = 18.5$  ksi). Using

the strain as the failure criterion, the maximum stress that can be applied for a given "failure strain" can be determined from Fig. 6 for different pulse durations. As expected, allowable maximum stress increases as the pulse duration decreases.

#### 4. COMPARISON WITH ASME CODE ALLOWABLE STRESSES

The use of linear elastic analysis and nonlinear elastic-plastic analysis for determining the response of a single degree of freedom system has been described in the previous sections. The elastic approach can now be used to determine the applied stress level at which the structure just reaches the code allowable stress. The elastic-plastic analysis can be used to determine the applied stress level to reach a strain of 0.75% ( $10\epsilon_y$  for the stress-strain curve used here). Figure 7 shows a comparison of the applied stress level to meet code allowable (yield stress for emergency conditions) and the stress for a maximum strain of 0.75% for different pulse durations. Even if failure is defined conservatively as reaching a strain of 0.75% the ratio between the code limit and failure is greater than four. The combined effect of inertia and material non-linearity is to introduce a substantial degree of conservatism when a structure is designed to code limits.

An alternate way to look at the safety margin using elastic-plastic dynamic analysis is to compare the static and dynamic reserve margins. The static reserve margin is defined as the ratio of the static load for failure (defined at 0.75% strain) to the static load to meet code limits. The dynamic reserve margin is defined as the ratio of the peak dynamic load to cause failure (0.75% strain as determined by elastic-plastic analysis) to the peak dynamic load to just reach code limits. Table I lists the static and dynamic reserve margins for different pulse durations calculated assuming 0.75% as the strain to failure.

It is seen that the dynamic reserve margin is significantly higher than the static reserve margin. Similar trends are also expected when the reserve margins are calculated assuming different strains to failure. The important conclusions that emerge from the margin calculations in Table I are as follows:

- When a structure is designed to meet the ASME Code the inherent safety margin to failure is significantly higher for short duration dynamic load pulses than for static load. This additional design margin is inherent in structures subjected to transient arising from events like earthquake, LOCA and SRV discharge.
- The higher safety margin for the pulse loads can be demonstrated by including effects of material non-linearity. When a pulse load is applied, the impulsive energy that is input depends not only on the magnitude of the applied load but also on the duration of the load pulse. As the duration of the pulse gets smaller, much higher applied loads can be tolerated since the energy for plastic deformation remains the same.

## 5. CONCLUSIONS

It is shown that the safety margin inherent in nuclear structures designed to meet ASME Code limits is significantly higher for dynamic pulse type loads than for static loads when effects of material non-linearity are included.

24308

TABLE 1

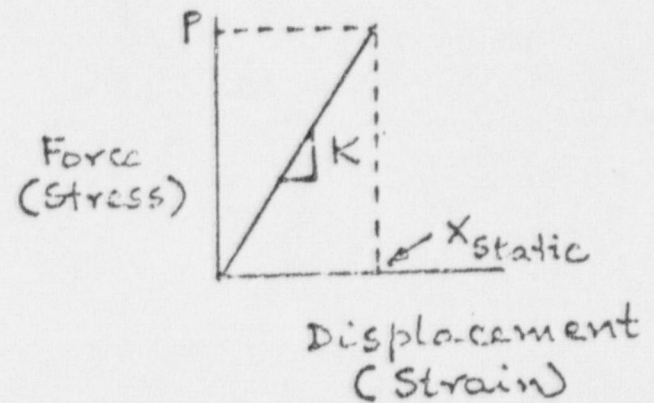
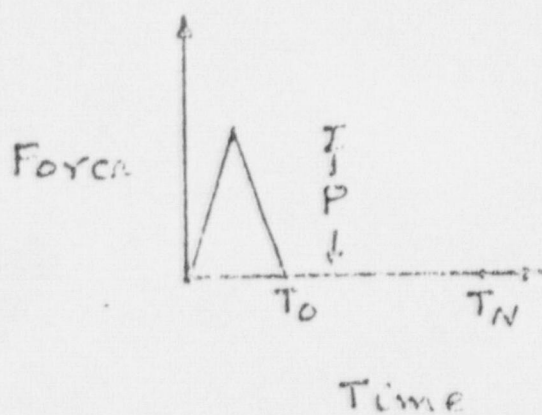
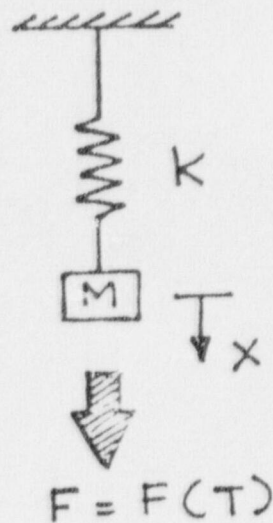
## RESULTS FOR SDOF SYSTEM SUBJECTED TO A TRIANGULAR PULSE

<u>Width of Pulse/ Natural Period of SDOF</u>	<u>Reserve Margin</u>		<u>Maximum Strain (<math>\epsilon_{\max}</math>)-%</u>	<u>Dynamic Reserve Margin/ Static Reserve Margin</u>
	<u>Static</u>	<u>Dynamic</u>		
0.1	1.15	4.52	0.75	3.93
0.2	1.15	4.52	0.75	3.93
0.3	1.15	4.47	0.75	3.89
0.4	1.15	4.34	0.75	3.77
0.5	1.15	4.23	0.75	3.68

For Service Level C, ASME Code allowable primary membrane stress limit at  $550^{\circ}\text{F} = S_y = 18.50 \text{ ksi}$   
(From Figure 4-1).

$$\text{Static Reserve Margin (at } \epsilon_{\max} = 0.75\%) = \frac{S(\epsilon_{\max} = 0.75\%)}{S_y} = \frac{21.25}{18.50} = 1.15$$

$$\text{Dynamic Reserve Margin (at } \epsilon_{\max} = 0.75\%) = \frac{\text{Peak load to produce 0.75\% strain by elastic-plastic analysis}}{\text{Peak load to just reach yield (linear elastic analysis)}}$$



$T_0$  = Pulse Duration

$T_N$  = Natural Period  
of System

FIG 1 Single Degree of Freedom Model  
(Elastic Analysis)

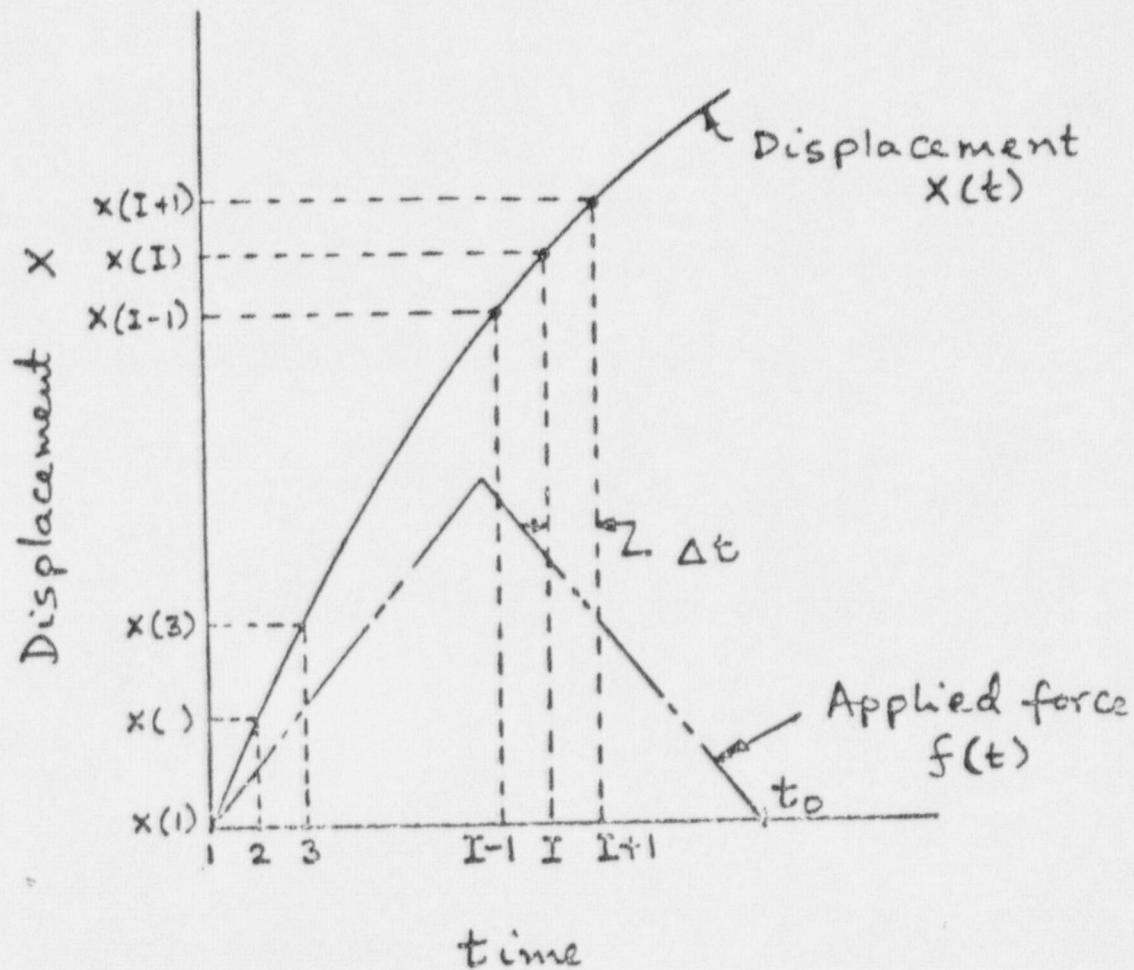


Figure 2. Numerical Integration Scheme

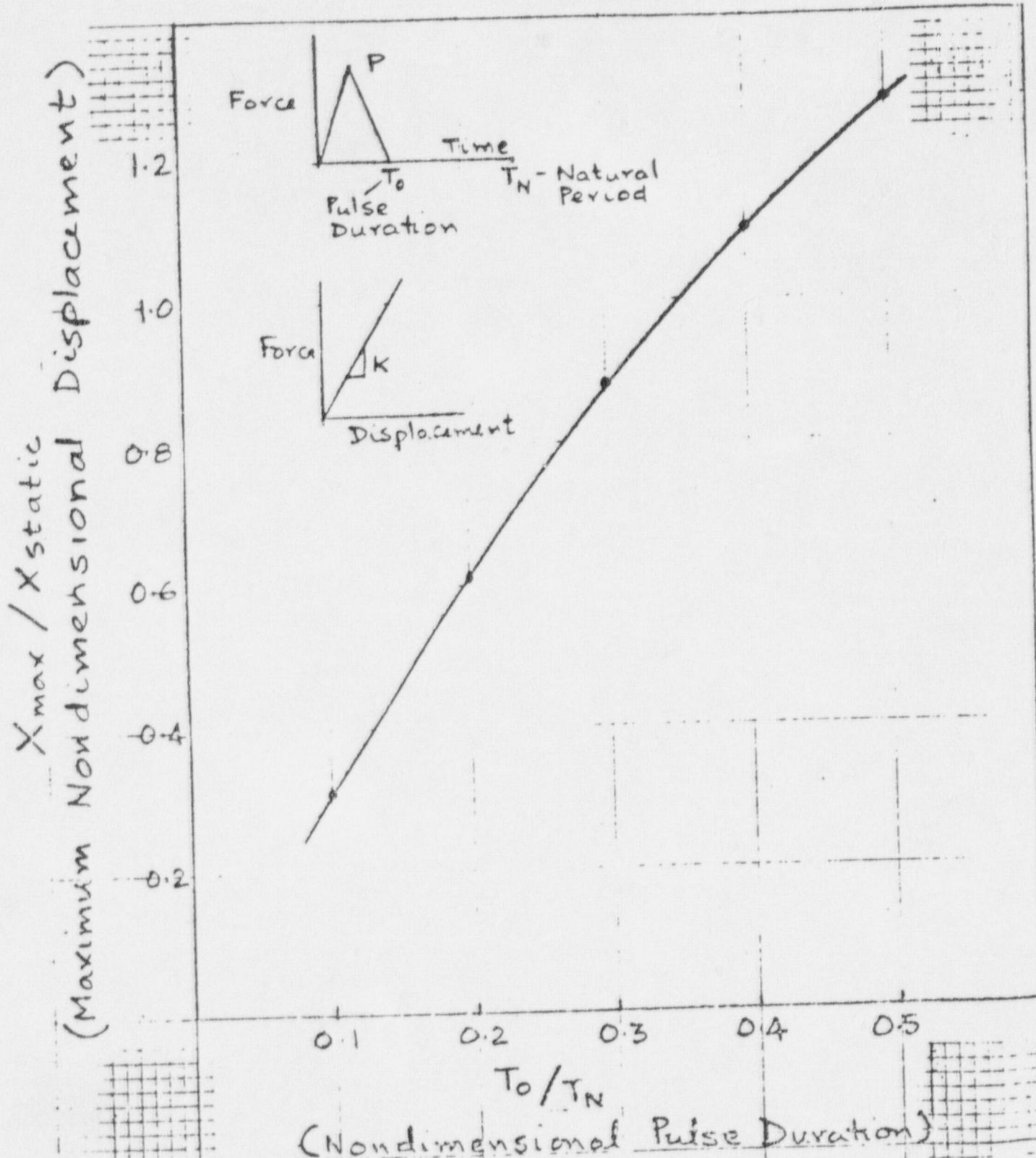


Fig 3 Maximum Elastic Response of a SDOF system for a Triangular Pulse

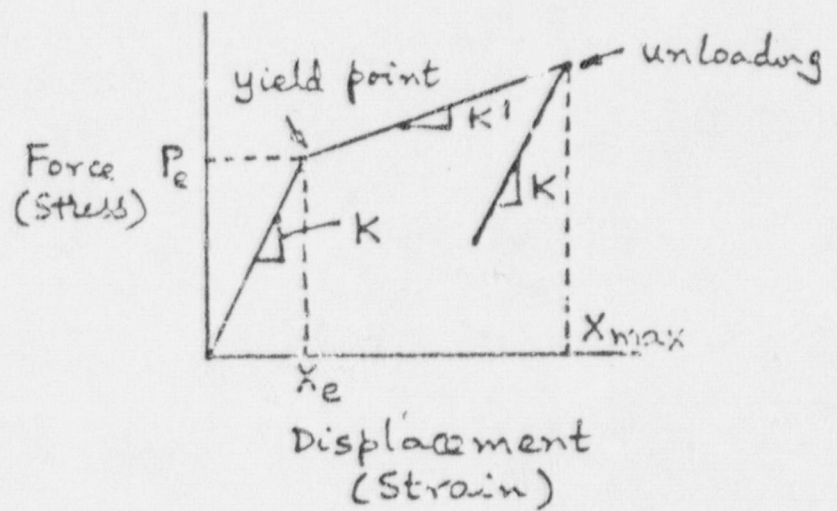
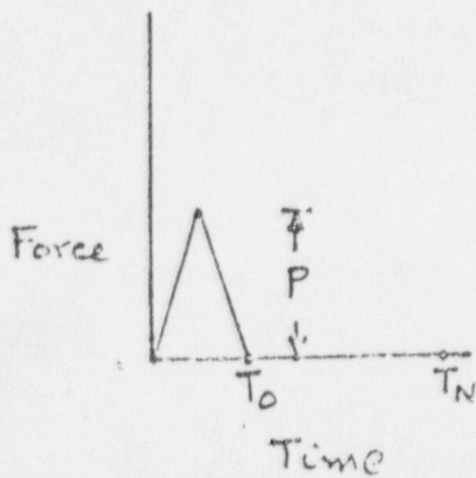
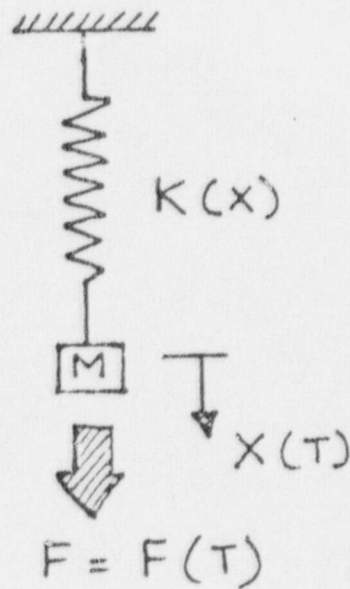


Figure 1 Single Degree of Freedom Model  
(Elastic - Plastic Analysis)

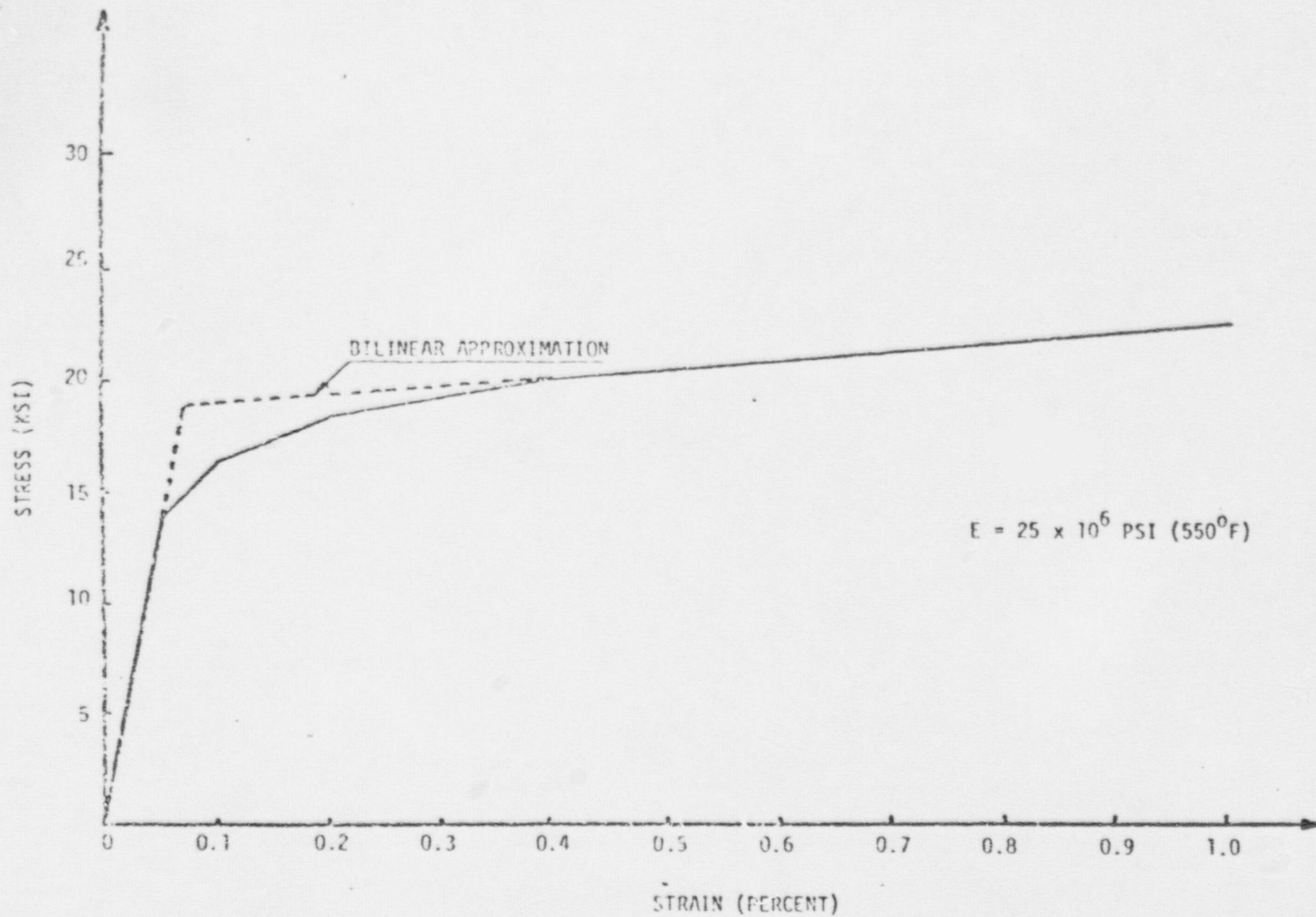
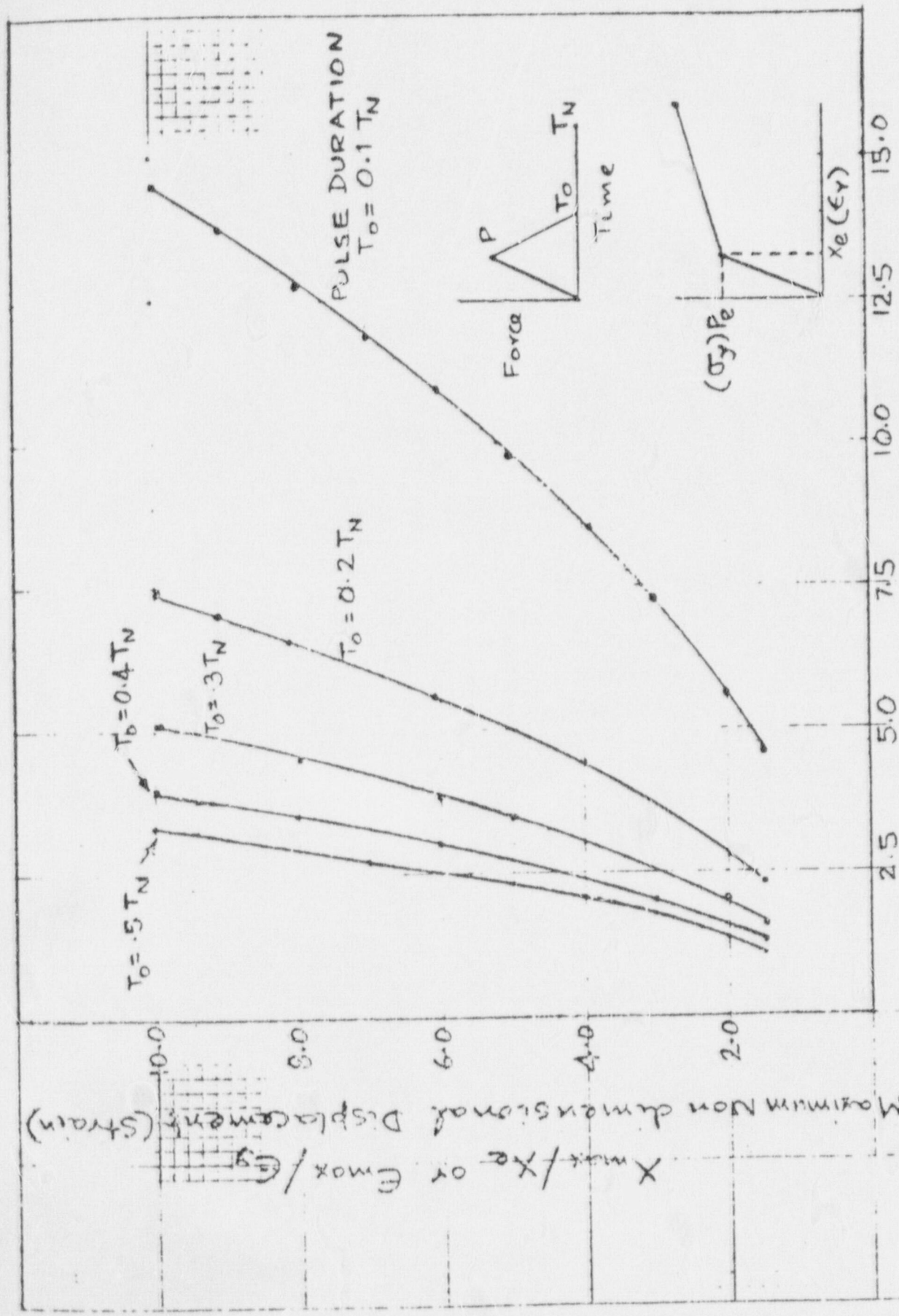


Figure 5 Code Minimum Stress-Strain Curve for 304 Stainless Steel at 550°F



Non-dimensional Peak Load (Applied Stress)

Maximum Elastic-Plastic Response of a SDOF System for Triangular Pulse Loading

Figure 6

Non-dimensional Applied Stress

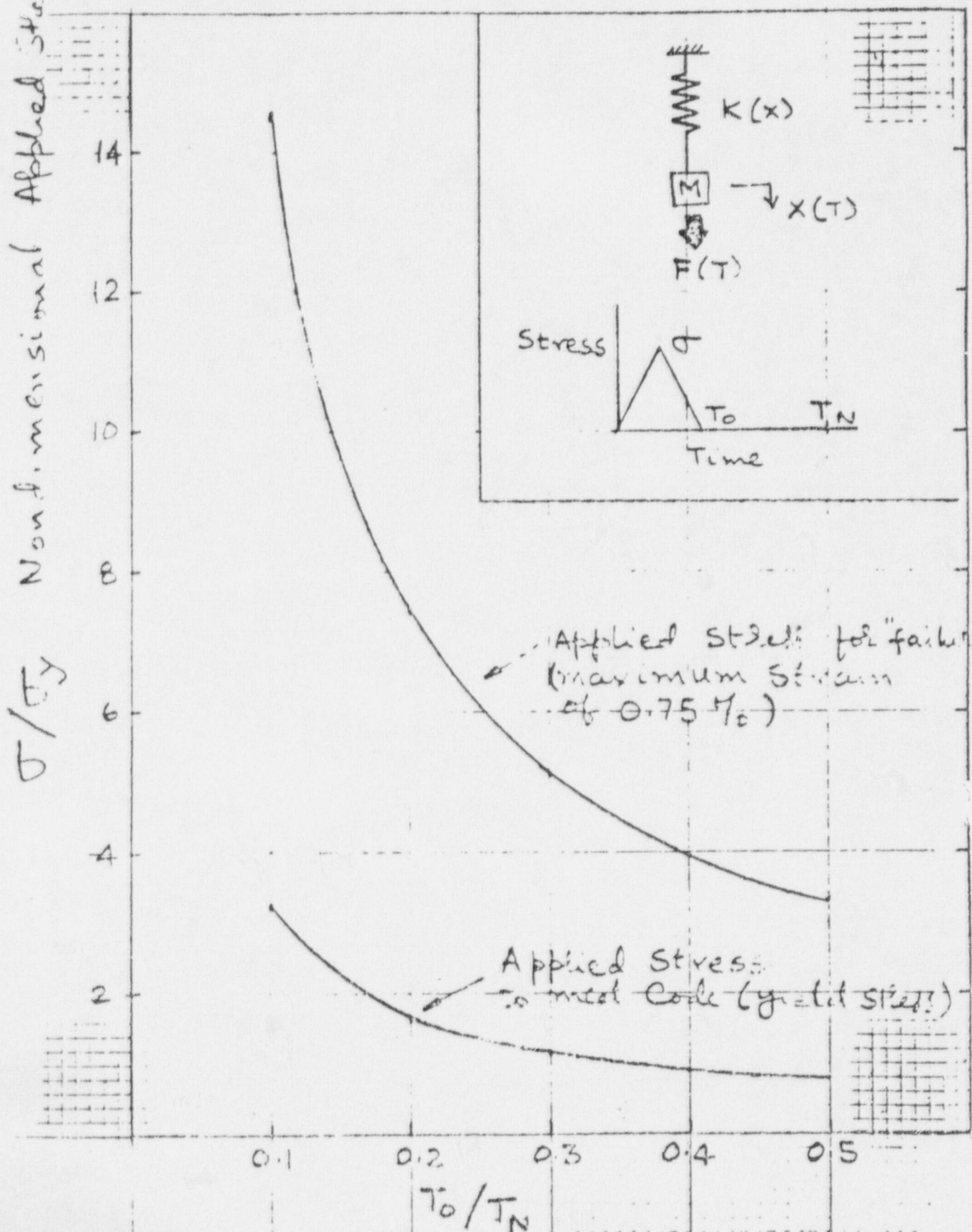


Fig. 7 Maximum Applied Stress to meet ASME Code limits and for failure (75% Stress)